3D dual-color PALM/dSTORM imaging of centrosomal proteins with nanometric resolution using MicAO 3DSR

Grégory CLOUVEL, Audrius JASAITIS and Xavier LEVECQ
Imagine Optic, 18 rue Charles de Gaulle, 91400 Orsay, France
contact@imagine-optic.com

APPLICATION NOTE

Summary

Photoactivation localization microscopy (PALM) and stochastic optical reconstruction microscopy (STORM) are becoming routine methods in biological imaging with optical resolution beyond the light diffraction barrier. We present MicAO 3DSR – the first adaptive optics device which introduces the three dimensional imaging capability for PALM/STORM. This apparatus, designed by Imagine Optic, contains the wave-front sensor and deformable mirror. With the help of these components MicAO 3D-SR corrects various types of aberrations, induced by optical elements inside the microscope and by the biological sample. MicAO 3D-SR optimizes the Point Spread Function (PSF) of the microscope and consequently improves the lateral localization precision of the PALM/STORM setup by 40%. In addition to that, MicAO 3D-SR brings in the ability to image fluorescent molecules in 3D. With its deformable mirror, it introduces controlled perfect astigmatism and allows us to precisely locate the position of fluorescing molecule in all three dimensions. In this application note we demonstrate the localization precision of PALM/STORM method when it is operated together with MicAO 3D-SR by 3D dual-color imaging of two proteins in centrosome – the cellular organelle which dimensions lye beyond the diffraction limit of 250x250x500 nm.

The nanometric resolution of intracellular components has become a necessary requirement in the field of fluorescence microscopy. The question of co-localization of proteins within cellular structures is very important in solving important biological problems. For example visualizing the structure of various adhesion complexes, the structure of nuclear pores, or the localization of different proteins in the cell membrane would help researchers to understand functional mechanisms. Unfortunately, the size of such structures usually lies beyond the diffraction limit and therefore they cannot be visualized in studies using today's widely popular fluorescence microscopy techniques.

Over the past five years, a number of super-resolution methods have emerged. These include structured illumination microscopy (SIM, Gustafsson, 2005), stimulated emission depletion microscopy (STED, Hell and Wichmann, 1994), photo-activation localization microscopy (PALM) and stochastic optical reconstruction microscopy (STORM) (Betzig *et al* , 2006; Hess *et al* , 2006; Rust *et al* , 2006). These methods overcome the diffraction limit obstacle in different ways and allow nanometric structures to be resolved (see for review Petterson *et al* l, 2010; Hell 2007, Huang *et al* , 2009). Their resolving power varies from 50-100 nm in SIM and approaches 10 nm in single molecule localization techniques such as PALM and STORM. Despite this superb lateral resolution, PALM and STORM methods are 2 dimensional because they cannot provide the precise axial information needed for 3-dimensional image construction. One way of qualifying a microscope's resolution is by measuring its Point Spread Function (PSF) and, because the PSF is symmetrical along the z axis, it is impossible to determine whether the point source is located above or below the focus. There are a number of ways to break the PSF's symmetry. The most notable methods include: inducing astigmatism using a cylindrical lens (Huang *et al* , 2008), creating a helical PSF (Quirin *et al* 2012) or employing the biplane method (Juette *et al*, 2008). Using these methods, the achieved z localization precision approaches 20-50 nm. The best axial resolution is provided by implementing an interferometric configuration of the PALM technique which reaches a z axis localization precision of 10-20 nm (Shtengel *et al*, 2009). Unfortunately, this method is very complex and difficult to implement.

In order to fully benefit from the resolving power of these single-molecule-detection techniques, it is very important to minimize the aberrations that arise in real-life situations. The microscope's components, the refractive index mismatch between the objective and the immersion medium, and the biological sample itself all introduce various types of aberrations. This results in a degradation of the PSF's quality which leads to a reduction in the number of detected photons and, ultimately, a reduction in resolution. To respond to this need, Imagine Optic has developed an adaptive optics device dedicated to PALM/STORM imaging called MicAO 3D-SR. This innovative, plug and play device employs a high-quality optical system that includes a wavefront sensor and a deformable mirror that, together, measure and correct for aberrations with extreme precision. The result is an increased amount of detected photons and an improved lateral localization precision in PALM/STORM method. Even more, MicAO 3D-SR can introduce small amounts of "perfect astigmatism" to provide 3-dimensional imaging capability similarly to cylindrical lenses. "Perfect astigmatism" provides a distinct advantage because the deformable mirror introduces astigmatism that is not contaminated by other aberrations, such that have been observed when using cylindrical lenses (Izeddin *et al* , 2012). The extremely high-quality PSF perfected by MicAO 3D-SR allows PALM/STORM microscopes to achieve lateral resolutions of 5-8 nm and axial resolutions of 10-16 nm in typical biological sample and typical conditions with the detection of 4000-1000 photons respectively (Figure 1). In order to demonstrate the localization precision of PALM/STORM methods if they are used together with MicAO 3D-SR, we performed two-color three-dimensional imaging of 2 fluorescently-labeled centrosomal proteins.

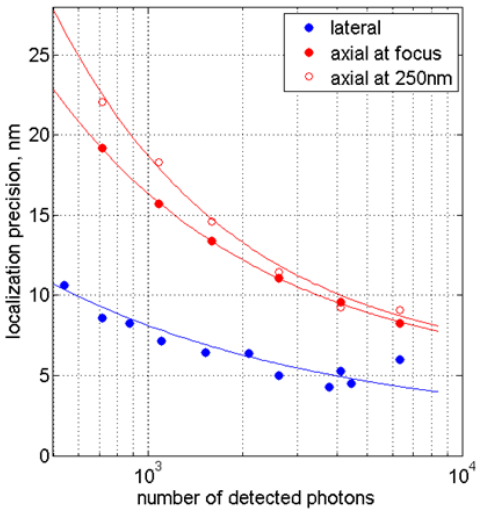

Figure 1. Localization precision dependence on the number of detected photons. Blue, lateral localization precision with optimized PSF and induced astigmatism; red filled circles, axial localization precision close to the focus; red empty circles, axial localization precision at + or - 250 nm away from the focus. The amplitude of astigmatism is 60 nm RMS. Solid lines are the fit of the data with a power law.

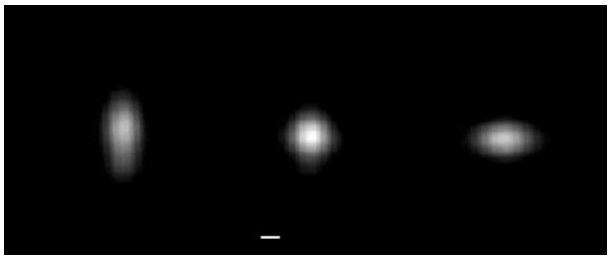

Figure 2. Image (averaged over 40 individual beads) of the PSF with 60 nm RMS astigmatism at -250 nm of the focus (left image), at the focus (center image), and at +250 nm of the focus (right image).

Centrosome plays an important role in many different cellular processes including the organization of microtubule arrays, cell cycle progression, the establishment of polarity of the cell and formation of primary cilium. One centrosome consists of two centrioles, which are barrel-shaped structures made of microtubules that are approximately 200 nm in diameter and 400–500 nm in length (Robbins *et al* ., 1968; Vorobjev and Chentsov Yu, 1982; Paintrand *et al* ., 1992). Despite the small size of centrioles, their structure is extremely complex. They are composed of hundreds of different proteins, which form so called pericentriolar matrix (PCM) or centrosomal matrix that is responsible for nucleating microtubules (Chretien *et al* ., 1997). Up to now, immuno-electron microscopy (immuno-EM) has been the only available technique to visualize centrosomal organization with the necessary accuracy since the dimensions of centrioles and their substructures are close to or below the diffraction limit (~250 nm). The main drawbacks of the immuno-EM technique are that it is expensive and time-consuming. Moreover, the available fixation techniques are not always compatible with preserving antigen accessibility. Therefore, super-resolution-fluorescence-microscopy techniques, such as PALM and STORM offer a promising alternative to immuno-EM.

Experimental procedures and results

Our PALM/STORM set-up was based on a standard epifluorescence microscope (Nikon Ti-E) equipped with an oil-immersion objective (Nikon Apo TIRF 100X, 1.49 NA). Epifluorescence excitation was provided by either a metal-halide lamp or a laser (405 or 561 nm) as explained in Izeddin *et al* (2012). MicAO 3D-SR was simply inserted into the emission pathway between the microscope and the EMCCD camera (Andor Ixon3 DU897).

During the installation of MicAO 3D-SR, we carried out a so-called closed-loop optimization in order to align the device and to perform the initial optimization of the microscope's PSF. To accomplish this, we used a sample containing fluorescent beads (1 µm diameter, red fluorescent beads (Invitrogen)). A 20-50 µl drop of diluted beads (10^{-2} dilution) was placed in the center of the cover slip and then washed twice with PBS so that only a small fraction of surface-immobilized beads was left. Next, PBS was added again and the specimen was placed into the microscope's sample holder. Then, we selected one bead in the field of view for the closed-loop procedure. The wavefront from the point source was precisely measured with the Shack-Hartman wavefront sensor (HASO-First) and immediately corrected by the deformable mirror (mirao 52-e). In this correction step, aberrations caused by the refractive index mismatch, the different optical elements inside the microscope and those of MicAO 3D-SR's components up to the deformable mirror were corrected. Because MicAO 3D-SR contains two more lenses after the deformable mirror, we corrected for those aberrations by using a 3N algorithm (Booth *et al* , 2002). In this last case, we used smaller, 100 nm diameter multicolor fluorescent beads (Invitrogen, 10^{-4} dilution) to fine-tune the PSF and to maximize the fluorescence signal. The final shape of the mirror after these corrections was then stored by the computer and used later as a starting reference point. These procedures had to be done once, during the installation of MicAO 3D-SR. There was no need to repeat them if the device was not physically moved and the ambient temperature remained stable.

Biological samples always introduce additional aberrations. To correct them, we started by introducing a small drop (20-50 µl) of 100 nm diameter multicolor fluorescent beads (Invitrogen, 10^{-5}-10^{-4} dilution) directly into the sample. We then washed the sample twice with

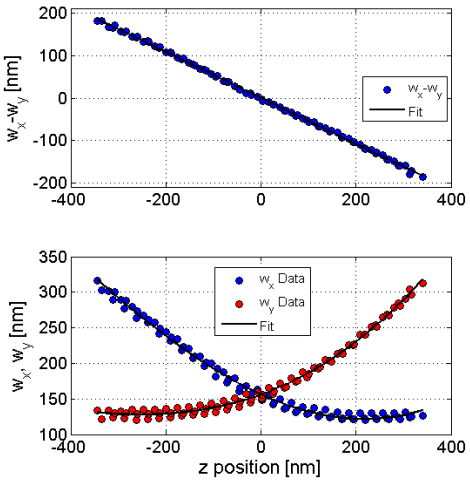

Figure 3. The calibration curve that is used for the determination of the location of the fluorophore along the z axis.

the specific buffer used for PALM/dSTORM imaging (Sillibourne *et al* , 2011). Note that it was important to have one or two beads in the field of view close to the region of interest. These beads were also used later for the lateral drift correction. We then reapplied the 3N iterative algorithm on the selected bead to correct for aberrations induced by the sample. We performed this optimization step separately for two different colors and thereby eliminated the influence of chromatic aberrations. The total effect of optimization of the PSF (closed and open-loop together) increased the amount of detected photons by 90% and improved the localization precision of PALM/STORM method by 40%.

For the 3-dimensional imaging, we introduced 60 nm RMS of perfect astigmatism using the deformable mirror thereby breaking the symmetry of PSF along the z axis. As such, it became extended along one direction in x-y plane when the point source was imaged above and in another direction when below the focal plane (Figure 2). This allowed us to determine the location of the fluorophore along the z axis and construct 3-dimensional images. We took a stack of 20 000 images for each color separately. The integration time of each frame was 30 ms and we collected on average 1500 photons/spot.

For the lateral position determination we fitted images with a 2D Gaussian function using an algorithm based on a modified Multi Target Tracking (MTT) algorithm (Sergé *et al* , 2008). This procedure returned the lateral coordinates of each fluorophore and also the dimensions of the diffraction limited spot along the x and y directions. These latter two parameters were used for the calculation of the axial location of the fluorophore. Separately, we constructed the calibration curve to determine the location of our bead along the z axis. For that, we moved the objective with a step of 24 nm and recorded a z-stack of a fluorescent bead. The 2D Gaussian fit of each image in the stack provided us with the depth-dependent amplitudes of the diffraction limited spot in x and y directions. An average of three calibration curves is shown in Figure 3. As can be seen, the calibration curve is symmetrical with respect to the focal point (Z=0 plane) and the noise level is of the same order above and below the focus, which again indicates the absence of aberrations in the sample and ensures the superb axial localization precision. The calibration curve allowed us to determine the localization of our fluorescent bead along the z axis.

To demonstrate the precision of PALM/STORM setup used together with MicAO 3D-SR we performed 3D 2-color imaging of two centrosomal proteins. The first attempt to do that in two dimensions was made by Sillibourne *et al*, 2011. The challenge of this experiment was to find cells where the centrosome would be properly oriented for the imaging since the angle of the sample with respect to the objective of the microscope was fixed. The authors established a HeLa cell line stably expressing mEos2-Centrin1 to enable the identification of centrioles. The

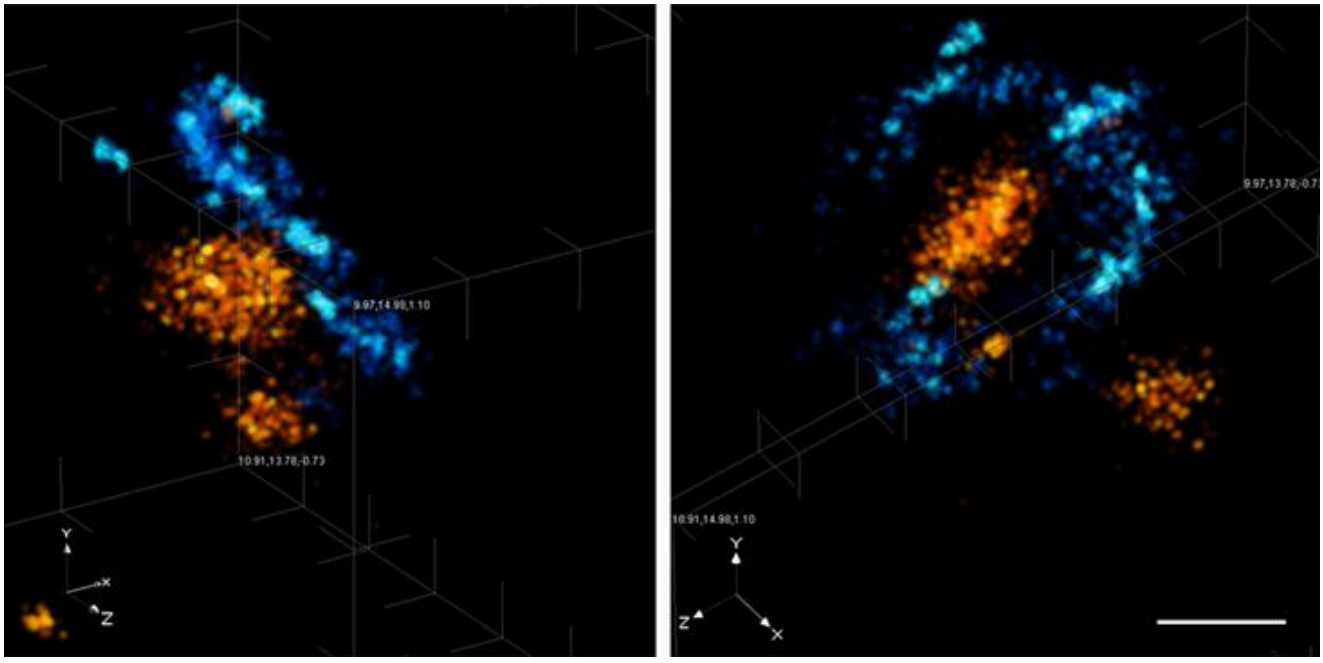

Figure 4. Combined two-color 3 dimensional PALM and dSTORM imaging of mEos2-Centrin1 (orange) and Alexa 647 labeled Cep164 (light blue). The scale bar is 200 nm. For visualization of results we used ViSP software (El Beheiry and Dahan, 2013).

Cep164 component of distal appendages was also chosen as a candidate for simultaneous dSTORM imaging because distal appendages of the mother centrioles are only a few nanometers in width and are challenging to image by immuno-EM. The HeLa mEos2-centrin1 cell line was labeled with an antibody to Cep164, stained with Alexa 647-conjugated secondary antibody and dual color two dimensional PALM/dSTORM imaging was performed (Sillibourne *et al*, 2011). In this application note, we present the dual-color 3-dimensional imaging of the same centriolar proteins using MicAO 3D-SR.

Two different orientations of the centrosome, imaged with 2-color 3-dimensional PALM/dSTORM using MicAO 3D-SR are shown in Figure 4. In this dataset, the average amount of photons detected from fluorophores was roughly 1500, providing us with 7 nm localization precision in the lateral and 13 nm in axial directions (Figure 1). Even at this scale, we still did not see overlapping points between two colors, which further demonstrates the precision of localization in this experiment. A striking observation is that the centrin staining in the mother–centriole appears tilted by about 40 degrees with respect to the distal appendage ring. In addition when a top view of the mother-centriole is observed (Figure 4, right), the centrin concentration seems elongated. This was already observed in similar view in 2D PALM/STORM (Sillibourne *et al*, 2011) but the 3D dataset suggests a more complex spatial distribution of intra-centriolar centrin than expected previously. Finally we observed that the Cep164 ring, which was not complete in this dataset, possibly due to technical reasons, was apparently composed of straight elements with a specific orientation, which could correspond to the distal appendages. Although much more work is needed with other centrosomal markers, including markers of the centriole wall, our preliminary results demonstrate the power of using PALM/STORM setup when it is operated together with MicAO 3D-SR.

Acknowledgements

This work was partially funded by the TRIDIMIC project (Agence nationale de recherche, ANR). We would like to thank James Sillibourne and Michel Bornens (Institute Curie, Paris) for sample preparations. We are grateful to Ignacio Izeddin and Xavier Darzacq (Ecole Normale Supérieure (IBENS), Paris), Maxime Dahan and Mohamed El Beheiry (Institute Curie, Paris) for their technical support and critical remarks concerning this application note.

Literature

- Betzig E, Patterson GH, Sougrat R, Lindwasser OW, Olenych S, Bonifacino JS, Davidson MW, Lippincott-Schwartz J, Hess HF. (2006) Imaging intracellular fluorescent proteins at nanometer resolution. *Science* **313**, 1642–1645.
- Booth MJ, Neil MAA, Juskaitis R, Wilson T (2002) Adaptive aberration correction in a confocal microscope. *PNAS* **99**, 5788-5792.
- Chretien D, Buendia B, Fuller SD, Karsenti E. (1997) Reconstruction of the centrosome cycle from cryoelectron micrographs. *J Struct Biol*, **120**, :117–133.
- El Beheiry M and Dahan M (2013) ViSP: representing single-particle localizations in three dimensions. *Nat. Met.* **10**, 689-690.
- Gustafsson MGL (2005) Nonlinear structured illumination microscopy: wide-field fluorescence imaging with theoretically unlimited resolution. *PNAS* **102**, 13081-13086.
- Hell SW and Wichmann J (1994) Breaking the diffraction resolution limit by stimulated emission: stimulated-emission-depletion fluorescence microscopy. *Opt. Lett.* **19**, 780-782.
- Hell SW. (2007) Far field optical nanoscopy. *Science*. **316**, 1153-1158.
- Hess ST, Girirajan TP, Mason MD. (2006) Ultra-high resolution imaging by fluorescence photoactivation localization microscopy. *Biophys J*. **91**, 4258–4272.
- Huang B, Wang J, Bates M, Zhuang X. (2008) Three-dimensional super-resolution imaging by stochastic optical reconstruction microscopy. *Science*, **319**, 810-813.
- Huang B, Bates M, Zhuang X. (2009) Super-resolution fluorescence microscopy. *Annu Rev Biochem*, **78**, 993-1016.
- Izeddin I, Beheiry ME, Andilla J, Ciepelewski D, Darzacq X, Dahan M (2012) PSF shaping using adaptive optics fro three-dimensional single-molecule super-resolution imaging and tracking. *Optics Express*, **20**, 4957-4967.
- Jones SA, Shim S-H, He J, Zhuang X. (2011) Fast, three-dimensional super-resolution imaging of live cells. *Nat. Methods*, **8**, 499-505.
- Juette MF, Gould TJ, Lessard MD, Mlodzianoski MJ, Nagpure BS, *et al* (2008) Three-dimensional sun-100 nm resolution fluorescence microscopy of thick samples. *Nat. Methods*, **5**, 527-529.
- Paintrand M, Moudjou M, Delacroix H, Bornens M. (1992) Centrosome organization and centriole architecture: their sensitivity to divalent cations. *J Struct Biol* **108**, 107–128.
- Petterson G, Davidson M, Manley S and Lippincot-Schwartz J. (2010) Superresolution imaging using single-molecule localization. *Annu Rev Phys Chem* **61**, 345-367.
- Robbins E, Jentzsch G, Micali A. (1968) The centriole cycle in synchronized HeLa cells. *J Cell Biol,* **36**, 329–339.
- Rust MJ, Bates M, Zhuang X. (2006) Sub-diffraction-limit imaging by stochastic optical reconstruction microscopy (STORM). *Nat Methods* **3**, 793–795.
- Sergé A, Bertaux N, Rigneault H and Marguet D. (2008) Dynamic multi-target tracing to probe spatiotemporal cartography of cell membranes. *Nat. Methods*, **5**, 687-694.
- Shtengel G, Galbraith JA, Galbraith CG, Lippincott-Schwartz J, Gillette JM *et al* . (2009) Interferometric fluorescent super-resolution microscopy resolved 3D cellular ultrastructure. *Proc. Natl. Acad. Sci. USA*, **106**, 3125-3130.

- Sillibourne JE, Specht CG, Izeddin I, Hurbain I, Tran P, Triller A, Darzacq X, Dahan M, Bornens M. (2011) Assessing the Localization of Centrosomal Proteins by PALM/STORM Nanoscopy. *Cytoskeleton* **68**, 619-627.
- Vorobjev IA, Chentsov Yu S. (1982) Centrioles in the cell cycle. I. Epithelial cells. *J Cell Biol,* **93**, 938–949.
- Quirin S, Pavani SRP, Piestun R. (2012) Optimal 3D single-molecule localization for super resolution microscopy with aberrations and engineered point spread functions. *PNAS*, **109**, 675-679.